Electronic Properties

DOI: 10.1002/anie.200701676

# Length-Dependent Band-Gap Shift of $TiO_3^{2-}$ Molecular Wires Embedded in Zeolite ETS-10**

*Nak Cheon Jeong, Myoung Hee Lee, and Kyung Byung Yoon**

Efforts have been directed at the synthesis and characterization of 1D quantum-confined semiconductor materials, since they have great potential to be widely used as building blocks for nanoscale electronic devices and other novel applications.[1–11] Of the 1D quantum-confined semiconductor materials, molecular wires are the thinnest.[1–5] However, examples of molecular wires are still very rare, and there is no method of synthesizing them in uniform diameters and controlled lengths. Accordingly, the relationship between the wire length ($l$) and the band-gap energy ($E_g$) in the quantum confinement region has not yet been determined for molecular wires, despite the fact that this relationship is crucial for the elucidation of the properties of the wires.

Zeolites are crystalline inorganic materials having nanometer-sized pores and channels with uniform shapes and sizes. These materials are widely used as catalysts, catalyst supports, adsorbents, ion-exchangers, and molecular sieves. ETS-10 ($Na_2TiSi_5O_{13}$) is a unique titanosilicate zeolite that contains regularly spaced 1D $TiO_3^{2-}$ molecular wires (-O-Ti(O-)$_4$-O-) with a diameter ($d$) of 0.67 nm. ETS-10 has two polymorphs: polymorth A (space group $P4_1$ or $P4_3$, not shown) and polymorph B (space group $C2/c$). The $TiO_3^{2-}$ molecular wires run along the [110] and [1$\bar{1}$0] directions (polymorph B, Figure 1) without touching each other.[12–15] Each $TiO_3^{2-}$ wire is surrounded by nanoporous silica with a pore size of $8 \times 5$ Å$^2$. In highly crystalline ETS-10, the lengths of the $TiO_3^{2-}$ molecular wires are greater than 25 nm.[16,17] Hence, it would be difficult to determine the $l$–$E_g$ relationship in the quantum confinement region unless the Bohr radius of the exciton in the molecular wire were to exceed 25 nm, since the quantum confinement effect ($E_g$ increases with decreasing $l$) is observed only in the region in which $l$ is smaller than the exciton Bohr radius.

[*] N. C. Jeong, Dr. M. H. Lee, Prof. Dr. K. B. Yoon
Center for Microcrystal Assembly
Center for Nanoporous Materials
Department of Chemistry
and Program of Integrated Biotechnology
Sogang University
Seoul 121-742 (Korea)
Fax: (+82) 2-706-4269
E-mail: yoonkb@sogang.ac.kr

[**] We thank the Ministry of Science and Technology (MOST) and Sogang University for supporting this work through the Take-Off Research and Internal Research Fund programs, respectively. We thank Prof. Hyeonsik Cheong and Hyunjin Lim for the Raman spectra. We also thank Jiyun Lee for preparing the illustrations.

Supporting information for this article is available on the WWW under http://www.angewandte.org or from the author.

The diameter of the $TiO_3^{2-}$ molecular wire in ETS-10 is comparable to that of a single-wall carbon nanotube ($d$ = 0.7 nm).[2] However, from the point of view of titanates, an important class of inorganic materials widely used in industry, the $TiO_3^{2-}$ molecular wire is ultimately the thinnest wire. Furthermore, no other molecular wires or nanorods have been produced in the form of a superlattice embedded in a chemically inert large-band-gap medium. ETS-10 can be produced in large quantities at low cost by hydrothermal synthesis.[12–15] Therefore, ETS-10 provides an unprecedented opportunity to systematically study the $l$–$E_g$ relationship of the titanate molecular wire and to explore the applications of molecular-wire superlattices as advanced materials.

Zecchina and co-workers, however, assumed that the band gap of the $TiO_3^{2-}$ wire in ETS-10 is independent of the length of the wire when the length is greater than 25 nm.[16,17] This assumption has been widely accepted by the community during the last decade.[18,19] The verification of its validity has not been possible owing to the inability to synthesize high-quality ETS-10 crystals of different sizes.[20] The standard approach to vary the size of a zeolite crystal is to vary the reaction time and temperature. Unfortunately, this standard approach has not worked for ETS-10. For instance, Southon and Howe demonstrated that, for a given synthesis gel, even a slight variation of the reaction time and/or temperature leads to ETS-10 crystals containing partially decomposed $TiO_3^{2-}$ molecular wires.[21] Furthermore, the decomposition of the $TiO_3^{2-}$ molecular wires yields titanium-containing amorphous or anatase nanoparticles whose absorption onsets appear at longer wavelengths.[22] Thus, the preparation of ETS-10 crystals of different sizes does not guarantee the successful elucidation of the $l$–$E_g$ relationship of the $TiO_3^{2-}$ molecular wires, unless the quality of the crystals is very high. Indeed, the UV absorption spectra reported for ETS-10 samples have not shown any correlation between the band-gap energy and the length of the crystals along the [110] direction ($L_{[110]}$; Figure SI-1 and Table SI-1 in the Supporting Information).[16,19–21] We now report an unprecedented and highly reliable method of synthesizing ETS-10 crystals of uniform sizes with average $L_{[110]}$ values of 0.3, 2, 5, 10, and 20 μm (denoted as E-0.3, E-2, E-5, E-10, and E-20, respectively).

The starting materials for our synthesis of ETS-10 were sodium silicate ($Na_2SiO_3$, 35 % $SiO_2$, 18 % $Na_2O$), [Ti($i$PrO)$_4$], $H_2SO_4$, NaOH, and KF. First, concentrated $H_2SO_4$ (4.5 g) was added to [Ti($i$PrO)$_4$] (5.7 g), and then distilled deionized water (35 g) was added. The mixture was boiled for a time period ($t$) of 5, 10, 15, 30, or 60 min. This procedure yielded anatase nanoparticles ($d$ = 2–5 nm) in an amount that increased with the value of $t$, namely, 0, 0.02, 0.08, 0.16, or 0.44 g (Figure SI-2). Independently, the silicon source was

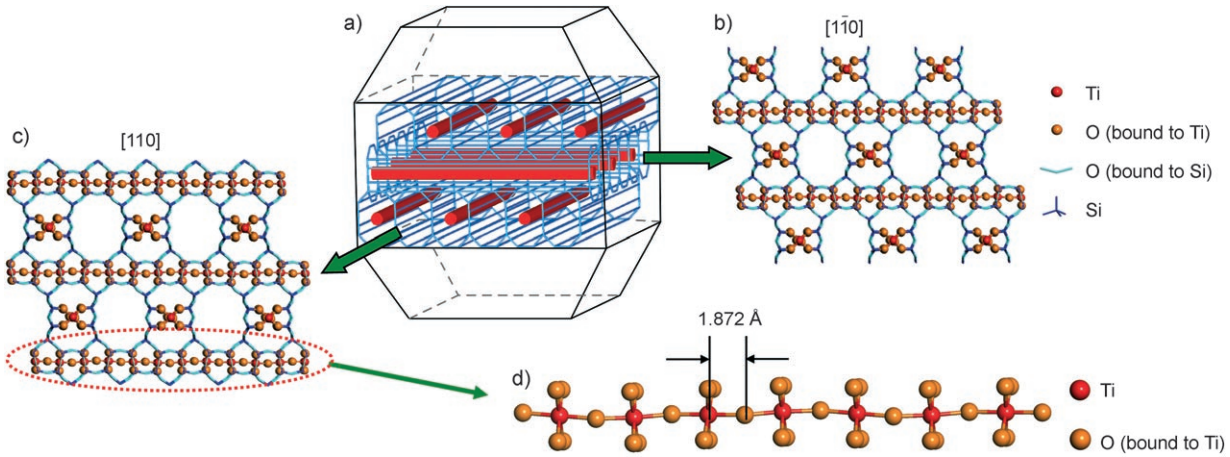


***Figure 1.*** Crystal structure of polymorph B of ETS-10. a) Typical truncated-bipyramidal morphology of the crystals, which consist of a three-dimensional network of $SiO_2$ channels (blue) and $TiO_3^{2-}$ molecular wires (red). b) View along the [1$\bar{1}$0] axis. c) View along the [110] axis. d) A single $TiO_3^{2-}$ molecular wire.

prepared by dissolving sodium silicate (18.3 g) in a dilute NaOH solution (2.6 g NaOH and 75 g water). A solution containing anatase nanoparticles was added to the silicon source, and a dilute KF solution (1.7 g KF and 15 g water) was subsequently added to the mixture. The mixture was aged for 18 h at room temperature and heated at 200 °C for 24 h.

The scanning electron microscopy (SEM) images (Figure 2) and powder X-ray diffraction (XRD) patterns (Figure 3 a) of the products confirmed that ETS-10 crystals were obtained and that the sizes of the crystals in each batch were fairly uniform. The sizes became highly irregular if the anatase nanoparticles were isolated prior to being used as titanium sources. Therefore, a key to the success of producing ETS-10 crystals of uniform sizes is to keep the freshly prepared anatase nanoparticles in the mother liquor and to

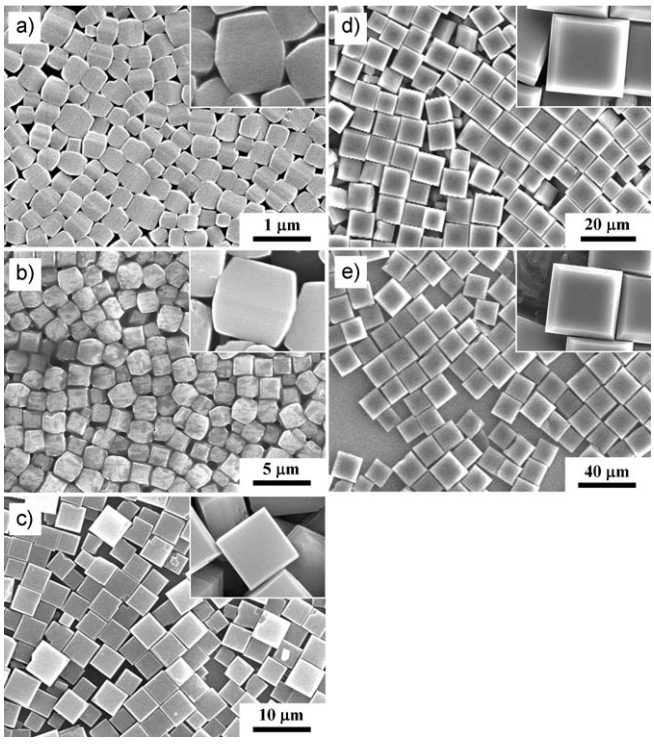


***Figure 2.*** SEM images of ETS-10 crystals with average lengths along the [110] direction ($L_{[110]}$) of a) 0.3 μm (E-0.3), b) 2 μm (E-2), c) 5 μm (E-5), d) 10 μm (E-10), and e) 20 μm (E-20). The images were obtained on a Hitachi S-4300 field-emission SEM at an acceleration voltage of 20 kV. The insets are higher-magnification images.

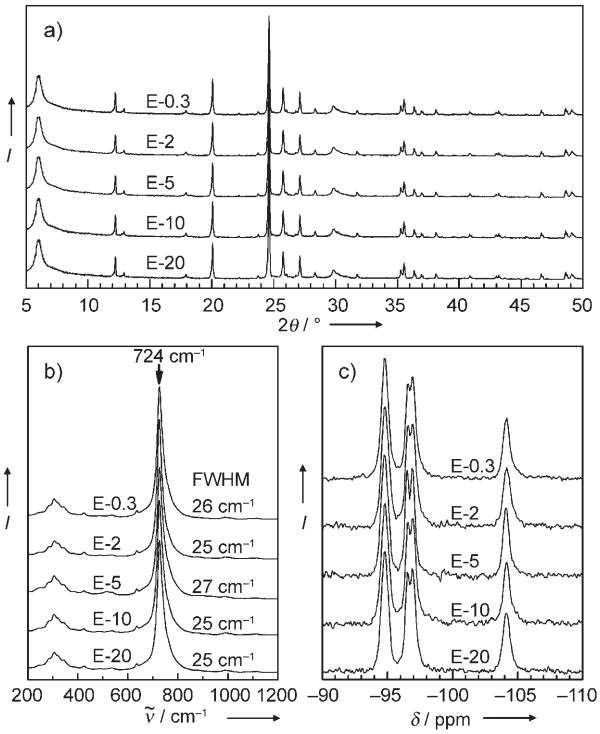


***Figure 3.*** a) Powder XRD patterns, b) Raman spectra, and c) solid-state MAS $^{29}Si$ NMR spectra of the ETS-10 samples. The XRD patterns were collected on a Rigaku D/MAX-2500/pc diffractometer. The Raman spectra were acquired using a 514.5-nm excitation beam from an $Ar^+$-ion laser. The NMR spectra were recorded on a Bruker DSX 400-MHz solid-state Fourier-transform NMR spectrometer at the Korea Basic Science Institute (Kyungpook National University).

  

use them in this form as titanium sources. None of the reported synthetic methods have adopted this methodology.[12–15,20–25] Another important discovery is that the average size of the ETS-10 crystals was inversely proportional to the amount of anatase nanoparticles produced in the solution (Figure SI-3).

The Raman spectra of the products are shown in Figure 3b. All the spectra have a sharp and strong peak at 724 $cm^{-1}$ with a band width (full width at half maximum (FWHM)) of 25–27 $cm^{-1}$. Other groups established that the 724 $cm^{-1}$ peak arises from the symmetric stretching of high-quality Ti-O-Ti chains and that the peak position shifts to significantly higher energy (to up to 820 $cm^{-1}$ [23]) as the crystal deteriorates.[20–24,26] The peak width for a high-quality ETS-10 crystal is approximately 25 $cm^{-1}$, and the width broadens (to up to 120 $cm^{-1}$) as the crystal deteriorates (Table SI-4).[21–24]

The solid-state magic-angle-spinning (MAS) $^{29}Si$ NMR spectra of the ETS-10 crystals (Figure 3c) showed resonance peaks at $\delta = -94.1$ (0.65), $-95.8$ (0.38), $-96.5$ (0.41), and $-103.3$ (0.60) ppm (the band widths are given in parentheses). The relative intensities of the peaks were 1.00:0.79:0.84:0.50, consistent with those reported by other groups for high-quality ETS-10 crystals. As the quality of the ETS-10 crystal degrades, the peaks at $\delta = -94.1$ and $-103.3$ ppm disappear, while those at $\delta = -95.8$ and $-96.5$ ppm coalesce because of broadening.[13,14,21–24]

The above results unambiguously show that all the crystals, regardless of their size, contain high-quality $TiO_3^{2-}$ quantum wires. High-resolution transmission electron microscope (TEM) images of the E-0.3 crystals showed that, over an area of $50 \times 50$ $nm^2$, pore coalescence occasionally occurs within the layers but not between the layers (Figure 4). This result indicates that most of the $TiO_3^{2-}$ quantum wires in the E-0.3 sample are longer than 50 nm.

Absorption spectra revealed the remarkable fact that the band-gap energy of the samples (estimated from the inflection point of the spectra) decreases with increasing $L_{[110]}$ value (Figure 5a and SI-5). The data of the $E_g$–$L_{[110]}$ plot shown in Figure 5b could not be fitted to the formula $E_g = A/L_{[110]}^2 + B$ (dotted curve), where A and B are chosen so that at least the two data points of E-0.3 and E-20 can fit into the formula. This result indicates that the average length of the $TiO_3^{2-}$ molecular wires is not linearly proportional to $L_{[110]}$.

Although not perfect, the effective-mass approximation has proven to be very useful for the analysis of the $l$–$E_g$ relationship of semiconductor nanorods.[6,7,16–18,27,28] Accordingly, we apply Equation (1), where $\Delta E_g$ is the difference

$$\Delta E_g = \frac{h^2}{4\mu_{xy} d^2} + \frac{h^2}{8\mu_z l^2} \quad (1)$$

between the $E_g$ value of the wire and that of a bulk three-dimensional titanate such as $MTiO_3$ (M = Ca, Sr, Ba), $h$ is the Planck constant, $\mu_{xy}$ and $\mu_z$ are the effective reduced masses of the exciton in the molecular wire along the perpendicular and axial directions, respectively, and $d$ and $l$ are the diameter and length of the molecular wire, respectively.

The forced fit of the $\Delta E_g$ value of each sample to Equation (1) with the assumption of an average wire length of

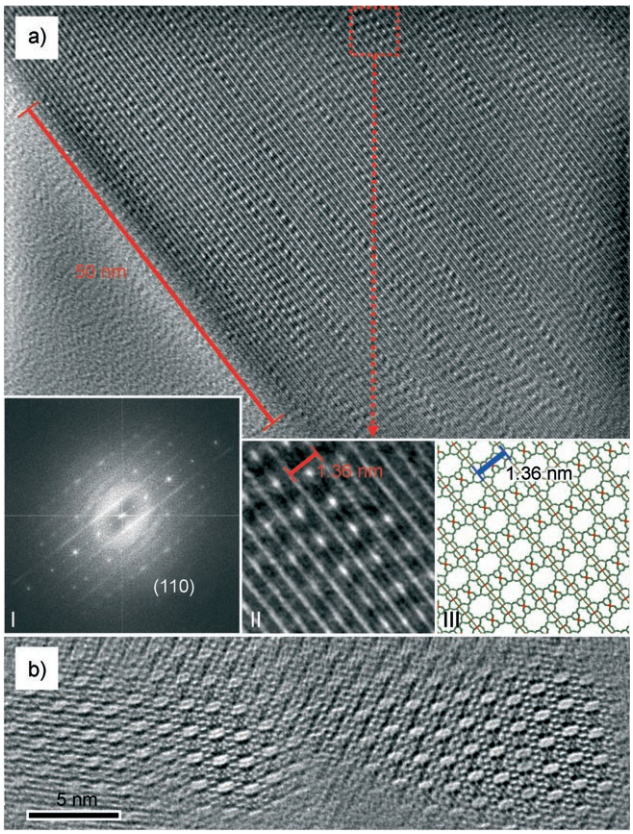


***Figure 4.*** a) TEM image of an ETS-10 crystal from sample E-0.3 at a magnification of 250000. Inset I: The corresponding fast Fourier-transform (FFT) image, which shows that the TEM image was taken perpendicular to the (110) face of the crystal. Inset II: An enlargement of the designated area in the TEM image. Inset III: Illustration of the ETS-10 structure viewed along the [110] axis. b) TEM image of the crystal at a magnification of 600000. The TEM images were collected on a JEOL JEM 4010 microscope.

50 nm for the E-0.3 sample (the minimum estimated length) and with $CaTiO_3$ ($E_g = 3.7$ eV) as the reference bulk material is shown in Figure 5c. This fit predicts $l$ values of 50, 57, 65, 83, and 167 nm, for the E-0.3, E-2, E-5, E-10, and E-20 samples, respectively. Furthermore, it predicts a $\mu_{xy}$ value of 15.2 $m_e$ and a $\mu_z$ value of 0.0006 $m_e$, which are the largest and the smallest values yet estimated. On the basis of these values, the electron mobility along the perpendicular direction is expected to be very low and that along the axial direction is expected to be very high, despite the oxide nature of the molecular wire.

The $\mu_{xy}$ value, which is derived from the height of the baseline in Figure 5c [the first term in Eq. (1)], can vary from 2.15 $m_e$ to 15.2 $m_e$, depending on the reference bulk material (rutile ($TiO_2$; $E_g = 3.03$ eV), anatase ($TiO_2$; $E_g = 3.18$ eV), $BaTiO_3$ ($E_g = 3.2$ eV), or $CaTiO_3$). The $\mu_z$ value may be much smaller if the $l$ value of the $TiO_3^{2-}$ molecular wire in E-0.3 is longer than 50 nm, which is also possible. If the $l$ value for E-0.3 is assumed to be as small as 25 nm, as estimated by others,[16–18] the $\mu_z$ value from the fit is 0.0027 $m_e$, which is still much smaller than the smallest values yet reported (for InSb, $\mu_z = 0.014\, m_e$,[29] for carbon nanotubes, $\mu_z = 0.019\, m_e$;[30] Table SI-6).

  

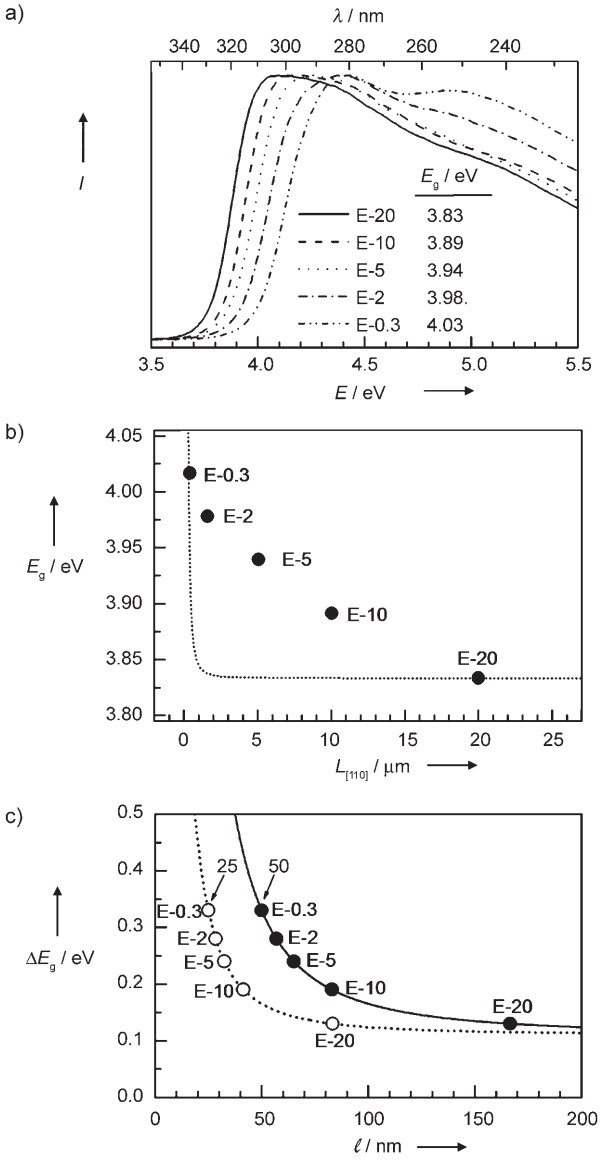


***Figure 5.*** a) The diffuse-reflectance UV-vis spectra of the ETS-10 samples, from which the band-gap energy ($E_g$) can be estimated (the intensities of the maximum absorption bands in the 290–330 nm region are normalized to an arbitrary Kubelka–Munk value). b) The dependence of the $E_g$ values of the samples on the average length of the crystals along the [110] direction ($L_{[110]}$). c) The forced fit of the relative band-gap energy ($\Delta E_g$; with respect to $CaTiO_3$) of the samples to Equation (1) for the cases in which the average length ($l$) of the $TiO_3^{2-}$ molecular wires in the E-0.3 sample is 25 nm or 50 nm. See text for details.

Such extraordinarily small $\mu_z$ values probably originate from the extraordinarily short Ti–O bond length (1.872 Å) along the axial direction.[15] This bond length is shorter than those of other Ti–O bonds involving six-coordinate titanium atoms, which range from 1.940 Å for rutile[31] to 2.005 Å for $BaTiO_3$[32] (Table SI-7). Stronger interatomic interactions give a smaller effective mass.[33] In this regard, the molecular wires in ETS-10 are unique, because such a short Ti–O bond length along the axial direction would not be possible outside of a zeolite framework, in which the strong spatial confinement imposed onto the molecules by the rigid zeolite framework does not exist.

The effective Bohr radius of the exciton along the axial direction ($a_{Bz}$) of the $TiO_3^{2-}$ molecular wire cannot be estimated, because the dielectric constant of the wire along the axial direction is not available. However, the very small $\mu_z$ value and the possibility of the dielectric constant being large (judging from the titanate nature of the wire; Table SI-6) suggest that the $a_{Bz}$ value could be larger than any known, thereby making it possible for the molecular wire to exhibit a length-dependent shift in the band-gap energy, *even at lengths much greater than 50 nm*. Consistent with this prediction, the $TiO_3^{2-}$ molecular wires do not fluoresce (even at 10 K), indicating a large spatial separation between the hole and electron wave functions in the excited state.[33]

We believe that our synthesis of high-quality ETS-10 crystals with different sizes and our subsequent elucidation of the long undiscovered $l$–$E_g$ relationship of the embedded $TiO_3^{2-}$ wires are important steps towards the development of quantitative mechanistic models for the remarkable phenomenon of the $TiO_3^{2-}$ molecular wire to exhibit a quantum confinement effect over such long wire lengths, towards the acquisition of direct evidence of the efficient electron transport predicted for the wires, and towards the application of the molecular-wire superlattices in nanoscale electronic devices. The high-quality ETS-10 crystals prepared could also be used as membranes for molecular separation.[34]

Received: April 16, 2007
Revised: May 13, 2007
Published online: July 2, 2007

**Keywords:** electronic properties · molecular wires · zeolites

[1] L. Venkataraman, C. M. Lieber, *Phys. Rev. Lett.* **1999**, *83*, 5334–5337.
[2] M. Ouyang, J.-L. Huang, C. M. Lieber, *Acc. Chem. Res.* **2002**, *35*, 1018–1025.
[3] J. H. Golden, F. J. DiSalvo, J. M. J. Fréchet, J. Silcox, M. Thomas, J. Elman, *Science* **1996**, *273*, 782–784.
[4] J. H. Golden, H. Deng, F. J. DiSalvo, J. M. J. Fréchet, P. M. Thompson, *Science* **1995**, *268*, 1463–1466.
[5] Y. Xia, P. Yang, Y. Sun, Y. Wu, B. Mayers, B. Gates, Y. Yin, F. Kim, H. Yan, *Adv. Mater.* **2003**, *15*, 353–389.
[6] S. Kan, T. Mokari, E. Rothenberg, U. Banin, *Nat. Mater.* **2003**, *2*, 155–158.
[7] L.-S. Li, J. Hu, W. Yang, A. P. Alivisatos, *Nano Lett.* **2001**, *1*, 349–351.
[8] S. P. Ahrenkiel, O. I. Mićić, A. Miedaner, C. J. Curtis, J. M. Nedeljković, A. J. Nozic, *Nano Lett.* **2003**, *3*, 833–837.
[9] H. Yu, J. Li, R. A. Loomis, L.-W. Wang, W. E. Buhro, *Nat. Mater.* **2003**, *2*, 517–520.
[10] Y. Huang, X. Duan, Y. Cui, L. J. Lauhon, K.-H. Kim, C. M. Lieber, *Science* **2001**, *294*, 1313–1317.
[11] X. Duan, Y. Huang, Y. Cui, J. Wang, C. M. Lieber, *Nature* **2001**, *409*, 66–69.
[12] S. M. Kuznicki, US Patent 4853202, **1989**.
[13] M. W. Anderson, O. Terasaki, T. Ohsuna, A. Philippou, S. P. MacKay, A. Ferreira, J. Rocha, S. Lidin, *Nature* **1994**, *367*, 347–351.

  

[14] M. W. Anderson, O. Terasaki, T. Ohsuna, P. J. O. Malley, A. Philippou, S. P. MacKay, A. Ferreira, J. Rocha, S. Lidin, *Philos. Mag. B* **1995**, *71*, 813 – 841.
[15] X. Wang, A. J. Jacobson, *Chem. Commun.* **1999**, 973 – 974.
[16] E. Borello, C. Lamberti, S. Bordiga, A. Zecchina, C. O. Areán, *Appl. Phys. Lett.* **1997**, *71*, 2319 – 2321.
[17] C. Lamberti, *Microporous Mesoporous Mater.* **1999**, *30*, 155 – 163.
[18] A. M. Zimmerman, D. J. Doren, R. F. Lobo, *J. Phys. Chem. B* **2006**, *110*, 8959 – 8964.
[19] V. Luca, M. Osborne, D. Sizgek, C. Griffith, P. Z. Araujo, *Chem. Mater.* **2006**, *18*, 6132 – 6138.
[20] B. Yilmaz, J. Warzywoda, A. Sacco, Jr., *Nanotechnology* **2006**, *17*, 4092 – 4099.
[21] P. D. Southon, R. F. Howe, *Chem. Mater.* **2002**, *14*, 4209 – 4218.
[22] Y. K. Krisnandi, E. E. Lachowski, R. F. Howe, *Chem. Mater.* **2006**, *18*, 928 – 933.
[23] L. Lv, J. K. Zhou, F. Su, X. S. Zhao, *J. Phys. Chem. C* **2007**, *111*, 773 – 778.
[24] C. C. Pavel, S.-H. Park, A. Dreier, B. Tesche, W. Schmidt, *Chem. Mater.* **2006**, *18*, 3813 – 3820.
[25] S. H. Noh, S. D. Kim, Y. J. Chung, J. W. Part, D. K. Moon, D. T. Hayhurst, W. J. Kim, *Microporous Mesoporous Mater.* **2006**, *88*, 197 – 204.
[26] S. B. Hong, S. J. Kim, Y. S. Uh, *Korean J. Chem. Eng.* **1996**, *13*, 419 – 421.
[27] M. L. Steigerwald, L. E. Brus, *Acc. Chem. Res.* **1990**, *23*, 183 – 188.
[28] Y. Kayanuma, *Phys. Rev. B* **1991**, *44*, 13085 – 13088.
[29] L. E. Brus, *J. Chem. Phys.* **1984**, *80*, 4403 – 4409.
[30] T. G. Pedersen, *Phys. Rev. B* **2003**, *67*, 073401.
[31] P. K. Naicker, P. T. Cummings, H. Zhang, J. F. Banfield, *J. Phys. Chem. B* **2005**, *109*, 15243 – 15249.
[32] Z.-X. Chen, Y. Chen, Y.-S. Jiang, *J. Phys. Chem. B* **2001**, *105*, 5766 – 5771.
[33] Y. Wang, N. Heron, *J. Phys. Chem.* **1991**, *95*, 525 – 532.
[34] H.-K. Jeong, J. Krohn, K. Sujaoti, M. Tsapatsis, *J. Am. Chem. Soc.* **2002**, *124*, 12966 – 12968.

  